

Improvement in the gelling properties of myofibrillar protein from the razor clam (*Sinonovacula constricta*) through phosphorylation and structural characterization of the modified protein

Qing Zhang¹, Yakun Hou¹, Xiaohan Liu, Jilu Sun, Xianghong Wang, Yaxin Sang^{*}

College of Food Science and Technology, Hebei Agricultural University, Baoding, China

ARTICLE INFO

Keywords:

Myofibrillar protein
Phosphorylation
Structural characterization
Gel properties

ABSTRACT

This study investigated the modification of myofibrillar protein (MP) from the razor clam through phosphorylation by using various phosphate salts, namely, sodium tripolyphosphate (STPP), sodium trimetaphosphate (STMP), sodium polyphosphate (STTP) and sodium pyrophosphate (TSPP), and their mechanisms of action for functional and gelling properties. Fourier transform infrared spectrometry (FTIR) showed that MP introduced phosphate groups during phosphorylation; these phosphates changed the secondary structure. Moreover, MP after phosphorylation led to an increase in solubility, which was more evident in the case of TSPP phosphorylation, leading to the improvement of gel properties. Therefore, TSPP was the phosphate with the best gel properties in the modification of MP, showing the highest phosphorus content, which resulted in better gelling properties owing to its relatively shorter chains. These results showed that phosphate was able to improve protein cross-linking through ion interactions and electrostatic interactions, which ultimately improved the gelling properties of the razor clam protein.

1. Introduction

The Razor clam (*Sinonovacula constricta*) is native to estuaries and mudflats in China and Japan. As an economically important marine bivalve, it is extensively aquafarmed in China along the seashore area from Liaoning to Fujian Province (Ye et al., 2022). The annual production of the Razor clam was 869,251 tons in 2020 (Zhang, Miao, & Kong, 2022). Razor clams are a famous seafood and have been traditionally consumed in China because of their high protein content (50 %) and richness in polyunsaturated fatty acids (Ran, Li & Yan, 2019). However, under normal refrigerated storage conditions, the short shelf life of fresh razor clams due to enzymatic and microbiological spoilage limits further expansion of their farming and further restricts razor farmer income increases. The processing of razor clams into value-added products such as seafood sausages or seafood meatballs is one of the routes for value addition to the razor clam industry. Myofibrillar protein (MP), comprising approximately 55–65% of the total protein, exerts a prominent influence on the gelation characteristics, which is an important functional attribute for food manufacturing (Wang et al., 2022). However, the poor gelling properties of razor clam protein are limiting

factors for the application of razor clam in gelling-based products (Chen, Ren, Zhang, Xiong, & Zhang, 2020). Therefore, the modification of razor clam MP to improve their gel properties is particularly important for the further development of value-added razor clam products.

Protein modifications include physical, chemical, and biological modifications. Compared with glycosylation or acylation-driven chemical methods, phosphorylation is considered a safer chemical modification method with no toxic products being produced during the process, which makes it an advantage to food industries (Wang, Yang, & Chen, 2019). Protein phosphorylation refers to the formation of C–O–P (carbon–oxygen–phosphorus) or C–N–P (carbon–nitrogen–phosphorus) covalent bonds; such bonds are formed between inorganic phosphorus and oxygen atoms from the hydroxyl group of serine, threonine and tyrosine or between phosphorus and nitrogen atoms from the amino group of lysine at specific sites of protein molecules (Hadidi, Jafarzadeh, & Ibarz, 2021). Fig. S1 demonstrates the process of esterification occurring between diverse phosphates and protein molecules. Sodium tripolyphosphate (STPP), sodium trimetaphosphate (STMP), sodium polyphosphate (STTP) and sodium pyrophosphate (TSPP) are commonly used phosphorylating agents in the

* Corresponding author.

E-mail address: yxsang1418@163.com (Y. Sang).

¹ These authors equally contributed to this work as the first author.

food industry (Thangavelu, Kerry, Tiwari, & McDonnell, 2019). These agents are easy to access and have enough reactive groups to interact with proteins; they can effectively conduct phosphorylation of protein molecules, improving their functionalities and gelling properties (Chen et al., 2020). A previous study revealed an increase in the complexity of beef MP gel, resulting in a more refined and organized microscopic surface of the gel with the addition of STPP, sodium hexametaphosphate (SHMP) and TSPP (Hu et al., 2021). Chen et al. (2020) mentioned that MP from mantis shrimp had increased electronegativity and solubility, reduced tryptophan fluorescence, and formed a more ordered and denser three-dimensional gel network after STPP treatment at pH 8.0 and 9.0. Although previous research has investigated the modification of MP structure and improvement of MP functionality under phosphate treatment, the current understanding regarding the influence of phosphate treatment on MP derived from the razor clam is constrained in scope. Thus, there is a need to explore the impact of structural changes and gel properties of MP from the razor clam during phosphorylation treatment.

Therefore, the current study aims to elucidate how four different phosphates (STPP, STMP, STTP and TSPP) modify the MP of the razor clam by their conformation changes (structures, sulfhydryl groups and disulfide bonds), aggregation behavior (solubility, particle size and microstructure), gelling properties (gel strength, water holding capacity, water distribution, and rheological properties) and the relationship between conformation changes and property improvement. The objective of this study is to provide an approach for enhancing the gel-forming properties of razor clam MP, subsequently broadening clam razor application in gel-based value-added products.

2. Materials and methods

2.1. Materials

Razor clam (*Sinonovacula constricta*) was purchased freshly from a local aquatic product market (Baoding, Hebei, China). The razor clam samples were immediately transported to the laboratory in an ice container and maintained at a temperature of 4 °C. The extraction of MP was conducted on the same day. Chemicals, namely, STPP, STTP, STMP, and TSPP, and markers (PR 10–250 kDa) were acquired from Sevenbio Co., Ltd. (Sevenbio, Beijing, China). Additionally, sodium chloride, sodium hydroxide and urea were acquired from Sigma Reagent Co., Ltd. (St. Louis, MO, USA).

2.2. Preparation of MP

The MP from the razor clam was extracted according to Yu et al.'s 2021 method with some modifications. First, the meat from the razor clam was combined with phosphate buffer solution A (20 mmol/L at pH 7.0) at 1:3 (w/v), homogenized by a homogenizer (JP-500C) for 1.5 min, and centrifuged at a temperature of 4 °C and a relative centrifugal force of 6790 g for a duration of 20 min. This precipitate was extracted again with buffer A one more time under the same conditions. Subsequently, the obtained precipitates were subjected to two rounds of rinsing with distilled water. After centrifuging and removing the water, the precipitates were added to phosphate buffer solution B (25 mmol/L at pH 7.0 containing 0.6 mmol/L NaCl) at 1:3 (w/v), homogenized for 1.5 min and centrifuged at a temperature of 4 °C and a relative centrifugal force of 6790 g for a duration of 20 min. After centrifugation, the supernatant was used for MP conformation changes and aggregation behavior studies. The precipitates were collected for gel preparation and characterization.

2.3. Phosphorylation of MP

MP suspensions (10 mg/mL) were formulated by dispersing the MP solution containing 2 % (w/v) STPP, STMP, STTP and TSPP (dissolved in

buffer B), followed by pH adjustment to 8.0, and then allowed to undergo a controlled reaction at a temperature of 40 °C for a duration of 2 h. After that, the suspensions were promptly transferred to an ice bath and kept for a duration of 30 min to inhibit any subsequent reactions. The reaction mixture was dialyzed with continuous magnetic stirring at a low temperature of 4 °C for 48 h to remove free phosphates. Then, the samples were freeze-dried for subsequent experiments.

2.4. Preparation of MP gel

An aliquot of 50 g MP and 4 mL phosphate solution (with a concentration of 6 % w/w) were combined at 40 °C for a duration of 2 h. After that, the mixture was subjected to heat treatment at a temperature of 40 °C for 30 min and a temperature of 85 °C for 40 min, followed by overnight cooling at 4 °C for subsequent analysis.

2.5. Determination of phosphorylation

The phosphorus content of protein was determined by the molybdenum blue colorimetric method (Jia et al., 2023). The MP samples were carefully digested in concentrated nitric acid (14.5 mol/L). The resulting digested product was then analyzed using a UV spectrophotometer, which served as an accurate measurement of the total phosphorus present in the sample. To determine the inorganic phosphorus content, a 2 mL sample was combined with 2 mL 10 % trichloroacetic acid. After centrifugation, the inorganic phosphorus of the supernatant was determined as the inorganic phosphorus content of the MP. Therefore, the phosphorylation content was determined utilizing the following mathematical equation:

$$\text{Phosphorylation} = \frac{W_P}{W_{MP}}$$

where W_P is the organic phosphorus content of the MP and W_{MP} is the MP mass.

2.6. Structural changes of phosphorylated MP

2.6.1. Sodium dodecyl sulfate–polyacrylamide gel electrophoresis (SDS–PAGE)

The SDS–PAGE experiment was conducted according to Yu et al.'s (2021) method. A solution of MP at a concentration of 5 mg/mL was combined with 25 μ L SDS–PAGE loading buffer (5 \times) and exposed to heat processing in a boiling water bath for 15 min at 100 °C. Afterward, 20 μ L of phosphorylated MP and untreated MP solutions were loaded onto a polyacrylamide gel electrophoresis system consisting of a 10 % separating gel and a 5 % stacking gel. The gel was subsequently stained to an electric current of 100 V. Following the electrophoresis process, the protein gels were subjected to staining with Coomassie Brilliant Blue for a duration of 30 min. Subsequently, the decolorized gels were imaged with a gel imager (Tanon-4600SF, Tanon Ltd., Shanghai, China).

2.6.2. Fourier transform infrared spectrometer (FTIR) analysis

One milligram of freeze-dried sample was mixed with 100 mg KBr, ground into powder, and then pressed into a 13 mm diameter disk in a dry environment (Chen et al., 2020). FTIR spectra of MP samples were acquired using an FTIR spectrometer (Thermo Scientific Nicolet iS20, US), in which the wavenumber range was from 500 to 4000 cm^{-1} .

2.6.3. Circular dichroism spectra

A CD (Applied Photophysics Ltd, JASCO810, UK) spectrometer was employed to determine the relative proportion of secondary structure in all samples. The MP samples underwent spectroscopic measurements with a step size of 1 nm and a scanning speed of 120 nm/min. The CD spectra obtained from these measurements allowed for the determination of the percentages of various protein secondary structures,

including α -helices, β -turns, β -sheets, and random coils.

2.6.4. Total sulfhydryl (SH) and free sulfhydryl (F-SH) contents

DTNB colorimetry was utilized to determine the content of sulfhydryl groups in MP (Ding et al., 2022). MP solution (1 mL, 1 mg/mL) was mixed in 5 mL of prepared solution (10 mmol/L ethylene diamine tetraacetic acid (EDTA), 8 mmol/L urea), and then, DTNB (100 μ L, 10 mmol/L) was added. The mixed solution was incubated for 20 min, and then the total sulfhydryl content was measured at 412 nm using a UV-Vis spectrophotometer N500.

For free sulfhydryl content detection, 5.5 mL of protein solution (1 mg/mL) and 100 μ L DTNB (10 mmol/L) were mixed, and the resulting mixture was subjected to spectrophotometric measurement to measure the absorbance at a specific wavelength of 412 nm.

$$\text{Sulfhydryl content } (\mu\text{mol/g}) = \frac{73.53 \times A_{412} \times D}{C}$$

where A_{412} represents the measured absorbance value at a wavelength of 412 nm. C represents the concentration of the protein (mg/mL), and D denotes the dilution factor.

2.7. General properties of phosphorylated MP

2.7.1. Particle size

The particle size was analyzed using a Malvern Zeta Sizer Nano ZS90 instrument (Malvern Instruments Ltd., Malvern, England). The sample was ultrasonically treated for 5 min before measurement (Geng, Xie, Wang, & Wang, 2021).

2.7.2. Protein solubility

The protein solubility was assessed employing the biuret assay, with bovine serum albumin serving as a standard (Wang, Xion, & Sato, 2017). The MP samples were centrifuged at a relative centrifugal force of 6790 g for a duration of 15 min. The protein solubility was determined utilizing the following mathematical equation:

$$\text{Protein solubility} = \frac{C_{\text{before}}}{C_{\text{after}}} \times 100\%$$

where C_{before} is the concentration of protein before centrifugation and C_{after} is the concentration of protein after centrifugation.

2.7.3. Morphological analysis by scanning electron microscopy (SEM)

After freeze-drying and gold coating, the surface morphologies of different MP samples were examined using SEM (Tescan MIRA LMS, Czech Republic) (Ding et al., 2022) at a magnification of 300 times.

2.8. Characterization of MP gel properties

2.8.1. Texture characteristics

The texture characterization of treated and untreated MP gels was measured by a texture analyzer apparatus (TMS-Pilot, FTC-mass spectrometer, USA). A controlled compression of 30 % was applied to the MP gel using a cylindrical probe, allowing for the assessment of texture properties. The experimental setup in the texture profile analyzer (TPA) involved configuring the instrumental settings. These settings included a load cell capacity of 500 N, a trigger force of 0.5 N, and a speed of 60 mm/s (Pan et al., 2018).

2.8.2. Water-holding capacity (WHC)

The WHC was resolved by measuring the percentage of water loss after centrifugation (Hu, Pereira, Xing, Zhou, & Zhang, 2017). Approximately 2 g of gel (W_1) was centrifuged at 8000g for 15 min, and the resulting weight (W_2) was measured. Triplicate analyses were conducted for each sample.

$$\text{WHC} = \frac{W_2}{W_1} \times 100\%$$

where W_1 is the weight of the sample before centrifugation and W_2 is the weight of the sample after centrifugation.

2.8.3. Low-field nuclear magnetic resonance (LF-NMR)

LF-NMR analysis was carried out following the method of Han, Wang, Xu, and Zhou (2014). The relaxation time and peak ratio were evaluated by utilizing an LF-NMR analyzer (MesoQMR23-060H-1, Suzhou Niumai Analytical Instrument Co., Suzhou, China), which operates at a magnetic field strength of 0.5 T at 23.2 MHz. T_2 was measured at 3000 ms and scanned every 8 s.

2.8.4. Dynamic rheological tests

Dynamic rheological tests were conducted by a high-precision rheometer (Anton Paar MCR 302, Austria). The MP solution samples were heated from 20 °C to 120 °C, with a controlled heating rate of 2 °C/min, and the storage modulus (G') and loss modulus (G'') were recorded (Zhu et al., 2022).

2.8.5. Interaction force

The molecular forces were measured abiding by a modified version of the methodology outlined in the provided description by Jia et al. (2023). The MP gel samples weighing 2 g were homogenized in different solutions: 0.05 M NaCl (S1), 0.6 M NaCl (S2), 0.6 M NaCl + 1.5 M urea (S3), 0.6 M NaCl + 8 M urea (S4), and 0.6 M NaCl + 8 M urea + 0.5 M β -mercaptoethanol (S5). The homogenized mixtures were then stirred at a chilled temperature of 4 °C for 1 h to allow the interactions to take place. Afterward, centrifugation was performed at a speed of 8,500 \times g for 15 min. The protein content was assessed through the biuret method, while the disparities in measurements between S2 and S1, S3 and S2, S4 and S3, and S5 and S4 were utilized to indicate the presence of ionic bonds, hydrogen bonds, hydrophobic interactions, and disulfide bonds, respectively.

2.9. Statistical analysis

Post hoc analysis using Duncan's test of ANOVA was conducted to identify significant differences by SPSS 22.0 (Chicago, USA). Significance was determined by a threshold of $p < 0.05$. All measurements were carried out in triplicate. Correlation between MP structure and their functional properties was analyzed using Pearson rank correlation analysis.

3. Results and discussion

3.1. Phosphorylation content

Fig. 1A illustrates the phosphorus content of the MP phosphorylated using different phosphates. The phosphorus content of treated MP was significantly increased compared to that of untreated MP ($p < 0.05$), showing that the effective incorporation of phosphate groups into MP was successful (Yan & Zhou, 2021). This was further confirmed by the findings from the FTIR analysis in Section 3.2.2. The phosphorus content in MP-TSPP was the highest (15.6 mg/g), followed by that in STTP (9.6 mg/g), STMP (12.7 mg/g), and STPP (14.0 mg/g) ($p < 0.05$), suggesting that TSPP exhibited the most pronounced binding efficiency with MP. It is worth noting that the average chain length of TSPP was the shortest among the phosphates used in this study (Fig. S1). Previous research has shown that the ability of phosphates to attach to proteins is related to their chain length (Hu et al., 2021). TSPP with a shorter chain length is more likely to attach to MP than other long chain phosphates, which could be the reason why MP treated with TSPP showed a higher phosphorylation content.

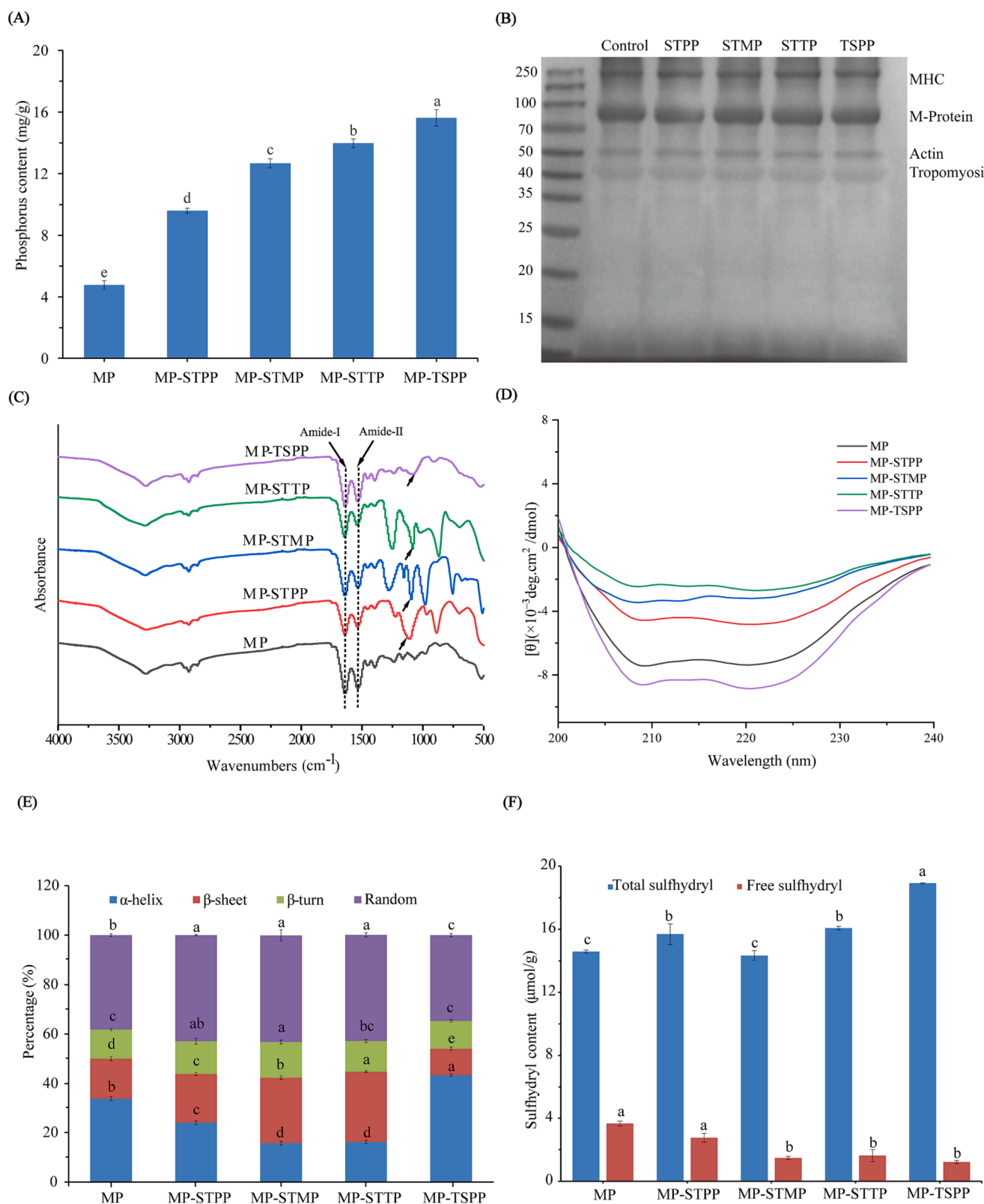


Fig. 1. Phosphorus content (A); SDS-PAGE profile of MP at different phosphates (B); FTIR spectra of MP samples at the wavenumber range of 4000–500 cm^{-1} (C); circular dichroism spectra (D); secondary structure (E); sulfhydryl contents (F) of MP samples. (MHC: myosin heavy chain). Groups with distinct alphabetic labels indicate statistically significant differences between the bars ($p < 0.05$).

3.2. Structural changes of phosphorylated MP

3.2.1. Sodium dodecyl sulfate–polyacrylamide gel electrophoresis (SDS–PAGE)

The changes in MP components are visually observed by gel electrophoresis, and the results of different phosphates on the primary structure are shown in Fig. 1B. The main proteins in razor clam MP are myosin heavy chain (MHC), M-protein, actin, and tropomyosin, with molecular weight values of 220 kDa, 97 kDa, 44 kDa and 37 kDa, respectively. The band intensities of MHC, M-protein, actin and tropomyosin changed nonsignificantly after phosphate treatment. The observed result aligned with the conclusions drawn by previous researchers (Hu et al., 2021). Moreover, the treated MP did not exhibit any additional bands in the observed spectra compared with the untreated groups (Fig. 1B), suggesting that the presence of phosphates did not result in the fragmentation or breakage of the peptide chains of MP.

3.2.2. Secondary structure

The FTIR technique has been extensively employed to investigate changes in protein functional groups (Sheng et al., 2019). The FTIR spectra depicted in Fig. 1C illustrate the spectral profiles of the untreated and treated MP. If the functional group is successfully modified, some characteristic peaks appear with the change in the original peak position or absorption intensity (Kobayashi, Mayer, & Park, 2017). Two distinct absorption bands were observed in the infrared region, namely, amide I and amide II, which were observed at wavelengths of 1645 cm^{-1} and 1537 cm^{-1} , respectively. The treated MP had no significant shift for amide I and amide II, indicating that there was no change with C=O stretching and N–H bending and C–N stretching (Han et al., 2022). In addition, a special absorption peak of phosphate groups was detected near 1110 cm^{-1} , such as the peak for the MP-STPP group at 1093 cm^{-1} , the peak for the MP-STMP group at 1095 cm^{-1} , the peak for the MP-STTP group at 1081 cm^{-1} , and the peak for the MP-TSPP group at 1083 cm^{-1} . They were assigned as P=O stretching. The results indicated that the protein reacted with the phosphate group, and the phosphate group was introduced to MP, which led to a change in the characteristic absorption of MP functional groups (Li, Sun, Ma, Jin, & Sheng, 2018). Phosphates can add phosphorus groups into proteins, which changes the structure of the protein, thus realizing the needed functional changes, such as gel, solubility and other capabilities.

The CD spectrum could reflect the conformational changes of MP after phosphorylation. In the CD spectrum of the treated MP, a single negative band was observed at approximately 208 nm, implying the predominant presence of an α -helix conformation due to the MP having a supercoiled α -helix structure (Fig. 1D). The distinct helical pattern was significantly enhanced at 208 nm after treatment with TSPP, suggesting an increase in the α -helix secondary structure. The secondary structure proportion of MP through relevant procedures was calculated (Fig. 1E). Compared with the untreated MP, the contents of α -helixes in the MP-STPP, MP-STMP and MP-STTP groups were reduced significantly ($p < 0.05$), while the contents of random coil and β -sheet structures were increased significantly ($p < 0.05$). Phosphates play a key role in controlling conformational transformation. However, the α -helix content in the MP-TSPP group significantly increased, and the β -sheet content decreased ($p < 0.05$). The presence of an increased proportion of random coil structures in the treated MP indicated a higher degree of stretching and disorder (Hu et al., 2022). However, compared with MP, the α -helix content of MP-TSPP was significantly increased. A high α -helix content would favor the stability and order of proteins. The predominant stability mechanism of the α -helix structure involves the formation of hydrogen bonds between the carbonyl oxygen (–CO) and the amino hydrogen (NH–) within the backbone of a polypeptide chain (Han et al., 2022). The above results demonstrated that phosphates rearranged and assembled the secondary structure of MP through hydrogen bonds.

3.2.3. Total sulfhydryl and free sulfhydryl content

The conformational changes occurring between free sulfhydryl and disulfide bonds have a pronounced influence on the structure and interactions of proteins (Liu et al., 2022). The samples with total and free sulfhydryl contents are illustrated in Fig. 1F. Compared with MP, the content of total sulfhydryl groups in MP-STPP, MP-STTP and MP-TSPP was significantly increased, and the content of free sulfhydryl groups in MP-STMP, MP-STTP and MP-TSPP decreased significantly ($p < 0.05$). This demonstrated that the addition of phosphate resulted in the uncovering of groups in the MP. Additionally, since the sulfhydryl group is converted to MP intermolecular or intramolecular disulfide bonds, amino acid residues from different parts of the same peptide chain or different peptide chains gather together, forming a more orderly arrangement of protein molecules in the network structure, thus causing protein cross-linking (Hu et al., 2021). In addition, different phosphates had different effects on MP; STPP had little impact on MP, while the greater change in MP-TSPP also indicated that TSPP reacted more fully with protein than the other three phosphates.

3.3. Aggregation behavior of phosphorylated MP

3.3.1. Size distribution

Particle size is a key factor in characterizing protein aggregation, which confirms the development of a compact and homogeneous gel structure (Liu et al., 2023). The untreated MP showed a multi-peak distribution (3 peaks), while phosphate-treated MP showed a double-peak distribution for MP-STPP, MP-STMP and MP-STTP and a single-peak distribution for MP-TSPP (Fig. 2A), indicating the uniform distribution of protein particles after phosphorylation. Fig. 2B illustrates the size distribution and mean particle size of the phosphorylated MP. In terms of particle size, untreated MP had a significantly larger size (1348.6 nm) compared to the treated MP, exhibiting the most diminutive particle size in the observations of MP-TSPP (255.83 nm) ($p < 0.05$). It might be that the phosphate group increased the charge aversion of MP and dissociated myofibril filaments in MP, which made the particle size of the treated MP smaller.

3.3.2. Solubility

Solubility, regarded as the most critical factor affecting protein functional features, is related to the capacity of proteins to dissolve or disperse in the initial solution (Hadidi et al., 2021). The solubility of treated MP with different phosphates is displayed in Fig. 2C. A comparison with the untreated MP revealed a considerable increase ($p < 0.05$) in solubility for all treated MPs, rising from 62 % to 81 %, suggesting that the involvement of phosphorylation was an effective strategy for enhancing the solubility of MP. Phosphate groups can attach to protein molecules, form hydrogen bonds with water molecules, and cause electrical repulsion between protein molecules (Hu et al., 2021). Therefore, the solubility of phosphorylated MP increased compared to that of the untreated group. In addition, phosphates with shorter chains possess a stronger attaching ability, which could form more hydrogen bonds with water molecules and give better solubility (Hu et al., 2021). The attachment of anionic phosphate groups dispersed the protein by increasing intermolecular repulsion, which was advantageous for the enhancement of protein solubility and protein dispersion (Li et al., 2018). Phosphoric acid groups could combine with water molecules to generate a significant quantity of hydrogen bonds, which was observed in this study.

3.3.3. SEM

Microstructural analysis of untreated and treated MP samples using SEM. Fig. 3 illustrates that untreated MP presented a sheet structure with an uneven distribution and size. The sheet structure of treated MP decreased, which aligned with the protein particle size results. This was because the implementation of negatively charged phosphate groups could destroy the complexation of proteins, resulting in a more compact

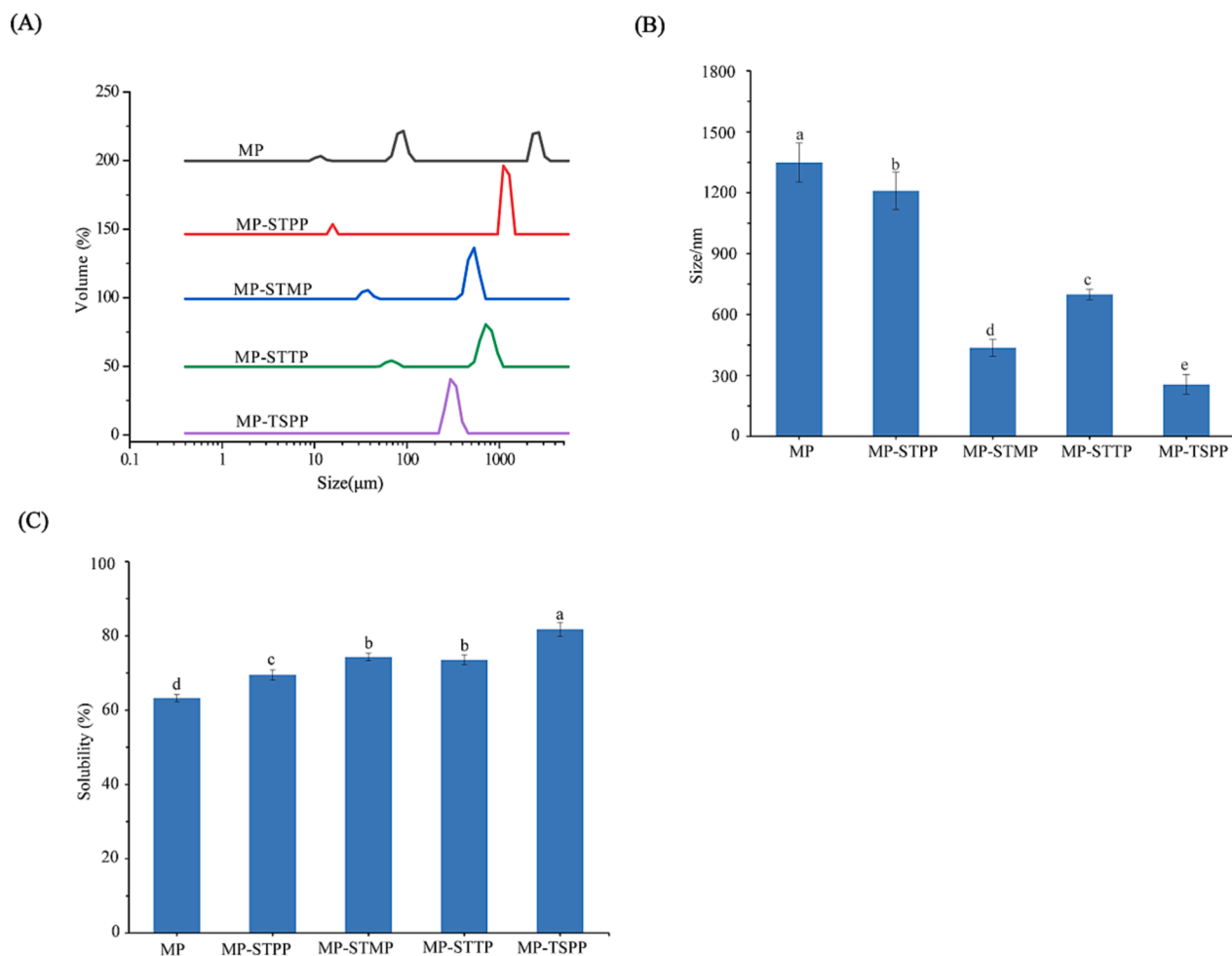


Fig. 2. Particle size distribution (A), mean particle size (B) and solubility (C) of MP samples. Groups with distinct alphabetic labels indicate statistically significant differences between the bars ($p < 0.05$).

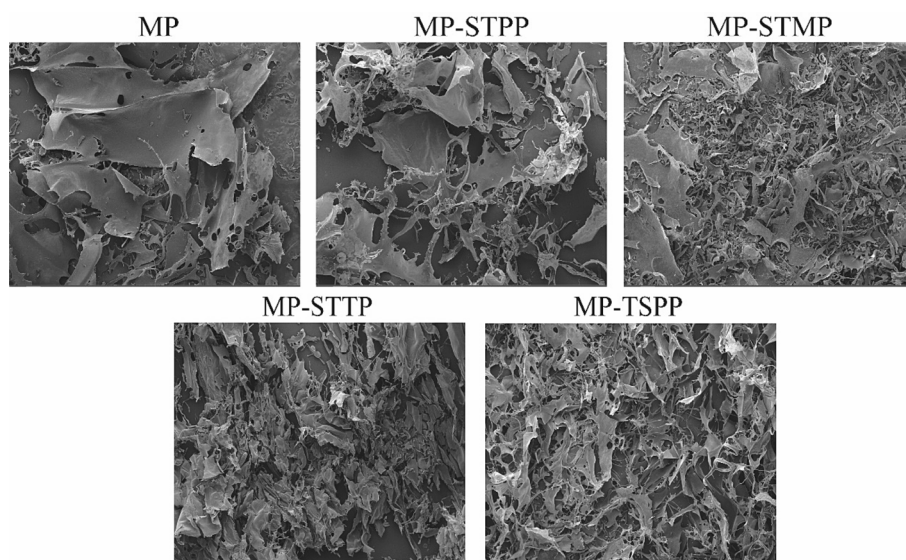


Fig. 3. Microstructure (magnification: 300 \times) of MP gel samples.

and even particle size (Hu et al., 2021). The small particle size promoted the protein-water interaction, as was determined with the solubility results (Wang et al., 2022). MP-TSPP had the most uniform and dense

microstructure, indicating that TSPP exhibited the highest efficacy in enhancing solubility and improving the structural attributes of the MP gel.

3.4. Characteristics of phosphorylated MP gel

3.4.1. Textural properties of MP gels treated with different phosphates

Table 1 presents a comprehensive overview of the textural characteristics of MP gels, focusing on four essential parameters: hardness, springiness, gumminess, and chewiness. These parameters are key indicators used to evaluate the quality and characteristics of protein gels. The gel hardness of MP was significantly increased for the MP-STMP, MP-STTP and MP-TSPP groups in comparison to the untreated MP gel ($p < 0.05$). The gumminess and chewiness of the treated MP gels displayed a similar trend as the hardness parameter, but the springiness did not exhibit a significant impact across the treatments with different phosphates ($p > 0.05$). TSPP demonstrated superior capacity in enhancing the textural characteristics of MP gel compared to other phosphates. On the one hand, it was possible that the creation of a three-dimensional gel network in the MP was influenced by the ionic interactions among the negatively charged phosphate groups and the positively charged $-\text{NH}_3^+$ groups of amino acids present in neighboring protein molecules (Jia et al., 2023). On the other hand, Wang, Yang, Fan, Zhang, and Chen (2019) reported that phosphate advanced the MP gel texture by increasing disulfide bonds, hydrophobic interactions and hydrogen bonds, leading to an amplification of the intermolecular interactions among protein molecules, consequently fostering the establishment of a more condensed and intricately structured gel network in three dimensions. The MP-TSPP gel showed the highest texture properties. Compared with other phosphates, TSPP has a higher phosphorus content and lower molecular weight, which dissociate or solubilize the myofibril more effectively (Julavittayanukul, Benjakul, & Visessanguan, 2006). Thus, it had a stronger effect on enhancing the texture of MP gels compared to other phosphates.

3.4.2. WHC of MP gels treated with different phosphates

WHC represents the ability to retain water within the protein gel network. It is related to the water retention capacity, including the hydration, solubility and hydrophobic interactions of MP (Chen et al., 2010). The impacts of phosphates on the WHC of MP gels are demonstrated in Fig. 4A. In contrast to the untreated MP gel, the treated MP gels exhibited a considerable increase ($p < 0.05$) in WHC, implying that the phosphorylation resulted in an enhanced ability to retain water during the gel formation phase. The added anionic phosphate groups were hydrophilic and could bind multiple water molecules (Chen et al., 2020).

3.4.3. Water distribution and mobility characterized by LF-NMR

LF-NMR can assess alterations in water distribution and migration by quantifying the relaxation time T_2 , which exhibits a strong link with WHC. In the NMR spectrum (Fig. 4B), the water population included three distinct peaks commensurate with the relaxation times T_{21} , T_{22} and T_{23} , which indicated bound water (T_{21}), immobilized water (T_{22}), and free water (T_{23}). T_{21} is closely associated with macromolecules and

Table 1
Effect of phosphates on texture characteristics.

Samples	Hardness (N)	Springiness (mm)	Gumminess (N)	Chewiness (mj)
MP	13.04 ± 0.73 ^d	6.46 ± 0.30 ^b	8.02 ± 0.72 ^d	51.78 ± 4.85 ^d
MP-STPP	13.68 ± 0.84 ^d	6.63 ± 0.29 ^{ab}	8.73 ± 0.86 ^{cd}	57.83 ± 4.79 ^{cd}
MP-STMP	17.39 ± 0.89 ^b	6.73 ± 0.13 ^{ab}	10.60 ± 0.36 ^b	69.96 ± 2.74 ^{ab}
MP-STTP	15.15 ± 0.99 ^c	6.34 ± 0.19 ^b	10.23 ± 0.78 ^{bc}	64.91 ± 6.54 ^{bc}
MP-TSPP	19.01 ± 1.23 ^a	7.00 ± 0.15 ^a	12.41 ± 1.35 ^a	78.34 ± 8.86 ^a

Note. All data were presented as mean values ± SD (n = 3). Different superscript letters in the same column of data indicate significant differences ($p < 0.05$).

represents only a minor part of the water. T_{22} is enclosed inside the MP gel matrix and is the predominant water component. T_{23} has high mobility and exists outside the gel network (Yu et al., 2022). When hydrogen protons are strongly associated with neighboring molecules or structures or when their movement is restricted (referred to as a smaller degree of freedom), the T_2 relaxation time is shorter (Han et al., 2014). As indicated in Table S1 and Fig. 4B, the T_{22} value of MP-TSPP exhibited a discernible decrease in relaxation time compared to MP, from 41.5 to 31.49 ms. With the exception of MP-STPP, T_{23} of the treated MP gels demonstrated a notable shift toward a shorter relaxation time direction, suggesting that TSPP had the capacity to alter the water status (T_{22} or T_{23}). We found that STPP, STTP and TSPP could increase P_{22} , while STMP otherwise decreased P_{23} , and STPP, STTP and TSPP could decrease P_{22} , while STMP otherwise increased P_{23} ($p < 0.05$). The relative composition percentage of water populations in MPs with forms of phosphates were also different (Shan et al., 2020). Phosphates enhanced the water-binding ability by increasing the ionic strength and facilitating stronger electrostatic interactions, leading to improved textural qualities in meat products (Shan, Li, Wang, Wang, & Kang, 2020). The phosphate-treated MP gels significantly increased the WHC.

3.4.4. Dynamic rheological

Dynamic rheological measurements are employed to evaluate the viscoelastic properties of the gels. The storage modulus (G') provides insight into the gel's elasticity, while the loss modulus (G'') reveals the gel's viscosity (Yu, Wang, et al., 2021). Fig. 4C and D show the storage modulus (G') and loss modulus (G'') changes with temperature for MP subjected to different treatments. The consistent observation of the storage modulus (G') being higher than the loss modulus (G'') suggested that the MP gels primarily exhibited elastic behavior. The MP gels that underwent the treatment showed a characteristic curve of storage modulus (G') with noticeable peaks occurring at approximately 64 °C, which were associated with the initial binding of denatured myosin heads, followed by the partial denaturation and unfolding of uncoiled myosin tails (Cao, True, Chen, & Xiong, 2016). The peak values of the treated MP gels were shifted to the right, implying that phosphorylation elevated the temperature at which myosin underwent denaturation. Additionally, the presence of different phosphates further enhanced the MP gelling elasticity, which was supported by the observed augmentation in the ultimate G' value. The presence of phosphoric acid groups in the phosphorylated MP might have contributed to the increased ionic interactions between the phosphorylated MP and positively charged chains, thus further enhancing the crosslinking of the MP gel (Jia et al., 2023). The phosphates developed an entangled protein network by exposing more active functional groups, such as disulfide bonds, which were converted by sulfhydryl groups participating in the gel formation process (Huang et al., 2019). Additionally, the final G' value in the MP-TSPP reached a maximum, which was increased by approximately 2 times, resulting in a stronger gel structure. The highest degree of phosphorylation additionally strengthened the interactions between proteins by enhancing ionic interactions. Similarly, Jin, Chen, Zhang, and Sheng (2020) reported that STPP and TSPP could effectively improve the network structure of egg white gel and that its G' value increased significantly with the addition of composite phosphate.

3.4.5. Interaction force

During the thermal-induced gelation of MP, the solubility of protein is used to characterize the gel force; the bonds involved include ionic bonds, hydrogen bonds, hydrophobic forces, and disulfide bonds (Ma, Wang, & Jiang, 2022). As shown in Fig. 4E, the predominant molecular forces responsible for retaining the network structure of the phosphorylated MP gel were determined to be hydrophobic interactions and disulfide bonds, which was similar to the findings obtained by Zhu et al. (2022). The phosphates markedly increased the hydrophobic force, ionic bond and disulfide bond of the MP gel ($p < 0.05$). In particular, the hydrophobic force and disulfide bond content of TSPP were increased by

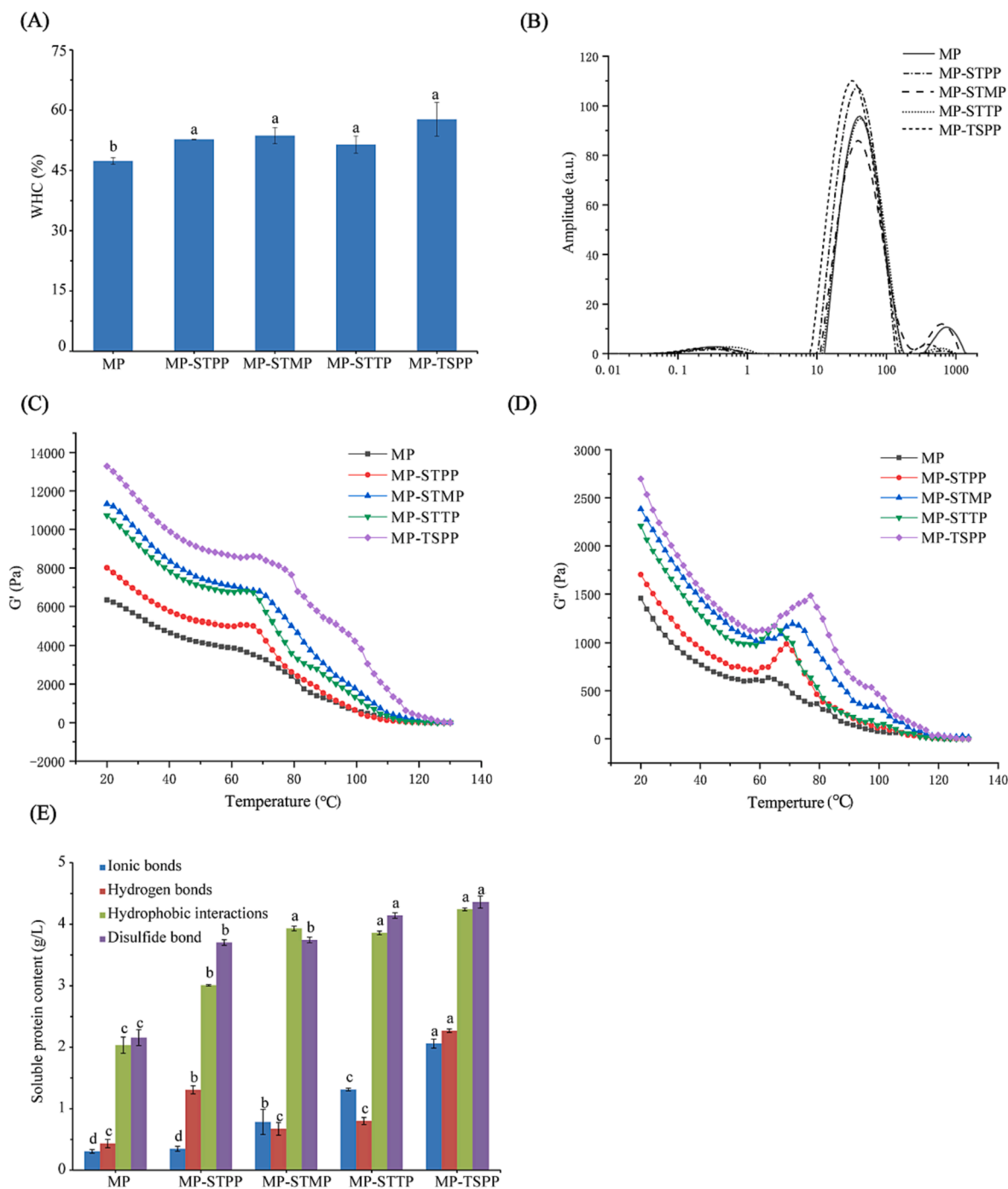


Fig. 4. WHC (A); and NMR (B); Storage modulus (G') (C); loss modulus (G'') (D) of MP samples; and molecular forces (E). Groups with distinct alphabetic labels indicate statistically significant differences between the bars ($p < 0.05$).

2 times. During MP heating, the system promotes protein cross-linking through disulfide bonds and hydrophobic interactions (Huang et al., 2019). This might be because the chelating ability between phosphates and metal ions promoted the expansion of proteins and improved the interaction between proteins, thus leading to an increase in molecular force. Furthermore, the hydrogen bonds of MP-TSPP and MP-STPP increased due to the stronger water binding capacity. The observed increase in ionic bonding could primarily be attributed to the ionic interactions among the negatively charged phosphate groups to the MP and the positively charged $-\text{NH}_3^+$ groups of amino acids in neighboring protein molecules, which was consistent with the degree of phosphorylation. The results of molecular forces well explained other indices of

MP, such as WHC and textural properties.

3.5. Correlation between MP structure and functional properties

Fig. 5A displays the correlation analyses investigating the connection between the structural characteristics and gel characteristics of razor clam MP. The color scheme in the figure assigns blue and red hues to negative and positive correlations, respectively, while the correlation coefficients span the range from -1 to 1 . The PC (phosphorylation content) of MP had a significantly positive correlation with solubility, gumminess, chewiness, hydrophobic force, and disulfide bond ($p < 0.05$). The superior quantity of PC indicated a better texture of the MP

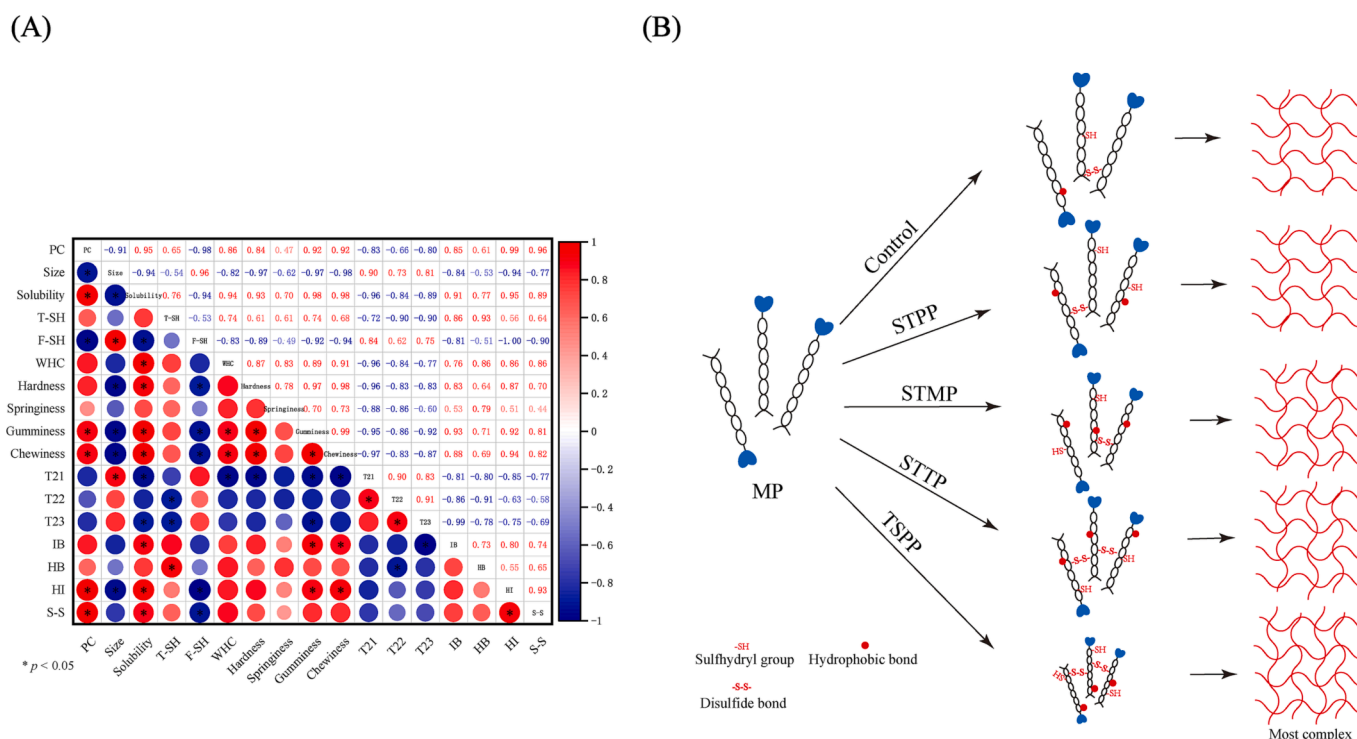


Fig. 5. Correlation analysis among the MP structure and MP gel properties, rheological properties (A); and proposed mechanism of STPP, STMP, STTP and TSPP of MP (B). Note: PC - phosphorus content; IB - ionic bonds; HB - hydrogen bonds; HI - hydrophobic interactions.

gel. However, the PC of MP exhibited a significant negative correlation with size and F-SH (free sulfhydryl content). The phosphate disrupted the structure of the protein, which resulted in a decrease in the size of F-SH. Moreover, particle size was negatively correlated ($p < 0.05$) with solubility, hardness, gumminess and chewiness, which illustrated that the decrease in size could promote the dispersion of MP in water and the formation of MP gel. Solubility was positively correlated ($p < 0.05$) with WHC, textural properties and intermolecular forces, which indicated that solubility was an important factor because it affected the gelation quality but also influenced other functionalities of the protein, including its gelation capabilities. The textural characteristics and WHC were two pivotal factors that governed the overall quality of the MP gel. The relationship between textural properties and WHC was extremely significant ($p < 0.05$). The enhanced textural properties of the gel network containing phosphate could be attributed to its compact structure, which restricted the movement of moisture and promoted moisture trapping. Intermolecular forces played a pivotal role in the establishment of a three-dimensional network in protein gel formation. Consistent with this result, the intermolecular forces of MP had a significantly positive correlation with textural properties ($p < 0.05$).

To enhance the comprehension of how phosphate positively influences gel quality, a diagrammatic illustration of the formation process of MP gels modified by different phosphates was proposed, as shown in Fig. 5B. The introduction of phosphates facilitated the linking and aggregation of proteins through the exposure of disulfide bonds and hydrophobic interactions, which resulted in improved gel elasticity, strength, and WHC outcomes. The phosphate groups improved the crosslinking of proteins and promoted protein network formation through ionic interactions. Meanwhile, after TSPP addition, MP exposed more hydrophobic bonds and disulfide bonds, resulting in a more intricate gel surface after the process of gelling. The effect of TSPP on MP was stronger than that on the others due to the shorter chain length.

4. Conclusions

This study provided information about how phosphates induce structural changes in MP and effectively enhance the functional characteristics of MP and MP gels. Four different phosphates, including STPP, STMP, STTP, and TSPP, were selected for MP phosphorylation. The phosphate functional group was successfully introduced to MP, which changed the MP conformation, increased the aggregation behavior and then further gave favorable gel properties. Phosphorylation significantly increased the phosphorylation content and further increased the number of hydrogen bonds, which gave the MP better solubility and reinforced the stability of the network structure in the protein gel. At the same time, the hardness of the gel was enhanced by phosphorylation, which formed a three-dimensional porous structure by decreasing the content of free water and the rheological properties of the protein gel. Moreover, all the results demonstrated that the MP gel treated with TSPP had the best performance, which was attributed to the relatively lower molecular weight and shorter chain length. The results indicated that phosphorylation by TSPP was an ideal way to modify razor clam MP for better functional properties.

CRediT authorship contribution statement

Qing Zhang: Conceptualization, Data curation, Formal analysis, Methodology, Writing – original draft. **Yakun Hou:** Formal analysis, Methodology, Writing – original draft, Writing – review & editing. **Xiaohan Liu:** Methodology, Writing – review & editing. **Jilu Sun:** Conceptualization, Writing – review & editing. **Xianghong Wang:** Conceptualization, Writing – review & editing. **Yaxin Sang:** Supervision, Writing – review & editing, Funding acquisition.

Declaration of Competing Interest

The authors declare that they have no known competing financial interests or personal relationships that could have appeared to influence

the work reported in this paper.

Data availability

The data that has been used is confidential.

Acknowledgements

This work was supported by the National Key R&D Program of China (2019YFD0902003) and Chunhui Talent Project Provincial Natural Science Foundation of Hebei, China (Grant No. C2022204154).

Appendix A. Supplementary data

Supplementary data to this article can be found online at <https://doi.org/10.1016/j.fochx.2023.101006>.

References

- Cao, Y., True, A. D., Chen, J., & Xiong, Y. L. (2016). Dual role (anti-and pro-oxidant) of gallic acid in mediating myofibrillar protein gelation and gel in vitro digestion. *Journal of Agricultural and Food Chemistry*, *64*(15), 3054–3061.
- Chen, J., Ren, Y., Zhang, K., Xiong, Y. L., & Zhang, D. (2020). Site-specific incorporation of sodium tripolyphosphate into myofibrillar protein from mantis shrimp (*Oratosquilla oratoria*) promotes protein crosslinking and gel network formation. *Food Chemistry*, *312*, Article 126113.
- Chen, C. G., Wang, R., Sun, G., Fang, H., Ma, D., & Yi, S. (2010). Effects of high pressure level and holding time on properties of duck muscle gels containing 1% curdlan. *Innovative Food Science & Emerging Technologies*, *11*(4), 538–542.
- Ding, Q. Y., Liu, X. H., Sang, Y. X., Tian, G. F., Wang, Z. X., & Hou, Y. K. (2022). Characterization and emulsifying properties of mantle proteins from scallops (*Patinopecten yessoensis*) treated by high hydrostatic pressure treatment. *LWT- Food Science and Technology*, *167*, Article 113865.
- Geng, F., Xie, Y. X., Wang, Y., & Wang, J. Q. (2021). Depolymerization of chicken egg yolk granules induced by high-intensity ultrasound. *Food Chemistry*, *354*, Article 129580.
- Hadidi, M., Jafarzadeh, S., & Ibarz, A. (2021). Modified mung bean protein: Optimization of microwave-assisted phosphorylation and its functional and structural characterizations. *LWT- Food Science and Technology*, *151*, 112–119.
- Han, G., Li, Y. X., Liu, Q., Chen, Q., Liu, H. T., & Kong, B. H. (2022). Improved water solubility of myofibrillar proteins by ultrasound combined with glycation: A study of myosin molecular behavior. *Ultrasonics Sonochemistry*, *89*, Article 106140.
- Han, M. Y., Wang, P., Xu, X. L., & Zhou, G. H. (2014). Low-field NMR study of heat-induced gelation of pork myofibrillar proteins and its relationship with microstructural characteristics. *Food Research International*, *62*, 1175–1182.
- Hu, Y. P., Zhang, L., Yi, Y. W., Solangi, I., Zan, L., & Zhu, J. (2021). Effects of sodium hexametaphosphate, sodium tripolyphosphate and sodium pyrophosphate on the ultrastructure of beef myofibrillar proteins investigated with atomic force microscopy. *Food Chemistry*, *338*, 128–146.
- Hu, H. Y., Pereira, J., Xing, L. J., Zhou, G. H., & Zhang, W. G. (2017). Thermal gelation and microstructural properties of myofibrillar protein gel with the incorporation of regenerated cellulose. *LWT- Food Science and Technology*, *86*, 14–19.
- Hu, Y. Y., Zhen, W., Sun, Y. Y., Cao, J. X., et al. (2022). Insight into ultrasound-assisted phosphorylation on the structural and emulsifying properties of goose liver protein. *Food Chemistry*, *373*, Article 131598.
- Huang, J. J., Bakry, A. M., Zeng, S. W., Xiong, S. B., et al. (2019). Effect of phosphates on gelling characteristics and water mobility of myofibrillar protein from grass carp (*Ctenopharyngodon idellus*). *Food Chemistry*, *272*, 84–92.
- Jia, B. B., Chen, J. Y., Yang, G. R., Bi, J. Y., Guo, J. T., et al. (2023). Improvement of solubility, gelation and emulsifying properties of myofibrillar protein from mantis shrimp (*Oratosquilla oratoria*) by phosphorylation modification under low ionic strength of KCl. *Food Chemistry*, *403*, Article 134497.
- Jin, H., Chen, J., Zhang, J., & Sheng, L. (2020). Impact of phosphates on heat-induced egg white gel properties: Texture, water state, micro-rheology and microstructure. *Food Hydrocolloids*, *110*, Article 106200.
- Julavittayanukul, O., Benjakul, S., & Visessanguan, W. (2006). Effect of phosphate compounds on gel-forming ability of surimi from bigeye snapper (*Priacanthus tayenus*). *Food Hydrocolloids*, *20*(8), 1153–1163.
- Kobayashi, Y., Mayer, S. G., & Park, J. W. (2017). FT-IR and Raman spectroscopies determine structural changes of tilapia fish protein isolate and surimi under different comminution conditions. *Food Chemistry*, *226*, 156–164.
- Li, P. S., Sun, Z., Ma, M. H., Jin, Y. G., & Sheng, L. (2018). Effect of microwave-assisted phosphorylation modification on the structural and foaming properties of egg white powder. *LWT- Food Science and Technology*, *97*, 151–156.
- Liu, X. H., Tian, G. F., Hou, Y. K., et al. (2023). Monosaccharide-induced glycation enhances gelation and physicochemical properties of myofibrillar protein from oyster (*Crassostrea gigas*). *Food Chemistry*, *428*, Article 136795.
- Liu, X. H., Mao, K. M., Sang, Y. X., Tian, G. F., Ding, Q. Y., & Deng, W. Y. (2022). Physicochemical properties and in vitro digestibility of myofibrillar proteins from the scallop mantle (*Patinopecten yessoensis*) based on ultrahigh pressure treatment. *Frontiers in Nutrition*, *9*, Article 873578.
- Ma, Y. Y., Wang, Y. H., & Jiang, S. S. (2022). Effect of gelatin on gelation properties of oyster (*Crassostrea gigas*) protein. *LWT- Food Science and Technology*, *158*, Article 113143.
- Pan, J. F., Jia, H. J., Shang, M. J., Xu, C., Lian, H. L., & Dong, X. P. (2018). Physicochemical properties and tastes of gels from Japanese Spanish mackerel (*Scomberomorus niphonius*) surimi by different washing processes. *Journal of Texture Studies*, *49*(6), 578–585.
- Ran, Z., Li, Z., Yan, X., et al. (2019). Chromosome-level genome assembly of the razor clam (*Sinonovacula constricta*) (Lamarck, 1818). *Molecular Ecology Resources*, *19*(6), 1647–1658.
- Shan, L. Y., Li, Y., Wang, Q. M., Wang, B. W., et al. (2020). Profiles of gelling characteristics of myofibrillar proteins extracted from chicken breast: Effects of temperatures and phosphates. *LWT- Food Science and Technology*, *129*, Article 109525.
- Sheng, L., Ye, S. Q., Han, K., Zhu, G. L., Ma, M. H., & Cai, Z. X. (2019). Consequences of phosphorylation on the structural and foaming properties of ovalbumin under wet-heating conditions. *Food Hydrocolloids*, *91*, 166–173.
- Thangavelu, K. P., Kerry, J. P., Tiwari, B. K., & McDonnell, C. K. (2019). Novel processing technologies and ingredient strategies for the reduction of phosphate additives in processed meat. *Trends in Food Science & Technology*, *94*, 43–53.
- Wang, K., Zhang, Y. M., Huang, M., Xu, X. L., Ho, H., & Sun, J. X. (2022). Improving physicochemical properties of myofibrillar proteins from wooden breast of broiler by diverse glycation strategies. *Food Chemistry*, *382*, Article 132328.
- Wang, X., Xiong, Y. L., & Sato, H. (2017). Rheological enhancement of pork myofibrillar protein-lipid emulsion composite gels via glucose oxidase oxidation/transglutaminase cross-linking pathway. *Journal of Agricultural and Food Chemistry*, *65*(38), 8451–8458.
- Wang, Y. R., Yang, Q., Fan, J. L., Zhang, B., & Chen, H. Q. (2019). The effects of phosphorylation modification on the structure, interactions and rheological properties of rice glutelin during heat treatment. *Food Chemistry*, *297*, Article 124978.
- Ye, W., Sun, H., Li, Y., et al. (2022). Greenhouse gas emissions from fed mollusk mariculture: A case study of a *Sinonovacula constricta* farming system. *Agriculture, Ecosystems & Environment*, *336*, Article 108029.
- Yan, C. J., & Zhou, Z. (2021). Solubility and emulsifying properties of phosphorylated walnut protein isolate extracted by sodium trimetaphosphate. *LWT- Food Science and Technology*, *143*(1–2), 111–117.
- Yu, W. Y., Wang, Z. M., Pan, Y. X., Jiang, P. F., et al. (2022). Effect of κ -carrageenan on quality improvement of 3D printed *Hypophthalmichthys molitrix*-sea cucumber compound surimi product. *LWT- Food Science and Technology*, *154*, Article 112279.
- Zhu, N., Zang, M. W., Wang, S. W., Zhang, S. L., Zhao, B., Liu, M., et al. (2022). Modulating the structure of lamb myofibrillar protein gel influenced by psyllium husk powder at different NaCl concentrations: Effect of intermolecular interactions. *Food Chemistry*, *397*, Article 133852.
- Zhang, M., Miao, Z., Kong, F., Xu, J., Ran, Z., Liao, K., et al. (2022). Effects of light intensity on artificial breeding of *Sinonovacula constricta*. *Aquaculture*, *558*, Article 738353.